Joint spectrum of photon pairs measured by coincidence Fourier spectroscopy

Wojciech Wasilewski

Instiute of Physics, Nicolaus Copernicus University, Grudziądzka 5, 87-100 Toruń, Poland, and Institute of Experimental Physics, Warsaw University, Hoża 69, 00-681 Warsaw, Poland

Piotr Wasylczyk

Institute of Experimental Physics, Warsaw University, Hoża 69, 00-681 Warsaw, Poland

Piotr Kolenderski and Konrad Banaszek

Instiute of Physics, Nicolaus Copernicus University, Grudziądzka 5, 87-100 Toruń, Poland

Czesław Radzewicz

Institute of Experimental Physics, Warsaw University, Hoża 69, 00-681 Warsaw, Poland

Received December 5, 2005; accepted January 16, 2006; posted January 20, 2006 (Doc. ID 66465)

We propose and demonstrate a method for measuring the joint spectrum of photon pairs via Fourier spectroscopy. The biphoton spectral intensity is computed from a two-dimensional interferogram of coincidence counts. The method has been implemented for a type-I downconversion source using a pair of common-path Mach–Zehnder interferometers based on Soleil compensators. The experimental results agree well with calculated frequency correlations that take into account the effects of coupling into single-mode fibers. The Fourier method is advantageous over scanning spectrometry when detectors exhibit high dark count rates leading to dominant additive noise. © 2006 Optical Society of America

OCIS codes: 270.5290, 190.4410, 300.6300.

Correlated pairs of photons are a popular choice in efforts to implement emerging quantum-enhanced technologies. Proof-of-principle experiments have demonstrated ideas such as quantum cryptography,[1] quantum clock synchronization,[2,3] quantum optical coherence tomography,[4] and one-way quantum computing.[5] In parallel with the expanding range of potential applications, the need to develop appropriate tools to engineer and to characterize sources of photon pairs is becoming apparent. Among various degrees of freedom describing optical radiation, the spectral one is essential to a number of techniques.[2–4] Also in other protocols, based on degrees of freedom such as polarization,[5] the spectral characteristics needs to be carefully managed in order to ensure the required multiphoton interference effects. This demand has brought a number of methods to control the spectral properties of photon pairs by engineering nonlinear media, the pumping and the collection arrangements.[6–10] A development that is needed to match these advances is the ability to diagnose accurately two-photon sources and to measure reliably their characteristics. An important work in this context is the recent application of scanning spectrometers to obtain joint spectra of photon pairs.[11]

In this Letter we demonstrate experimentally two-photon Fourier spectroscopy as a method to measure the joint spectrum of photon pairs. The setup is based on two independently controlled Fourier spectrometers in the common-path configuration. Such an arrangement guarantees the long temporal stability necessary to characterize weak sources of radiation operating at single-photon levels. We show that the two-dimensional map of coincidence counts recorded as a function of delays in the two interferometers can be used to reconstruct the joint spectrum of photon pairs. We present a measurement for a type-I spontaneous downconversion process in a bulk β-barium borate (BBO) crystal and compare the results of the reconstruction with theoretical predictions.

An idealized scheme of the experimental method is presented in Fig. 1. The source (X) produces nondegenerate pairs of photons in distinct spatial modes represented by diverging lines. Each photon is sent into a separate interferometer, where it is divided by beam splitter BS into two wave packets subjected to a delay difference τ_A and τ_B for photons A and B. The two wave packets interfere at beam splitter BS, and light emerging from the output of the interferometer is detected. A coincidence event is recorded if both photons reach their respective detectors. The quantity of interest is the coincidence probability $P_{AB}(\tau_A, \tau_B)$ measured as a function of the delays τ_A and τ_B.

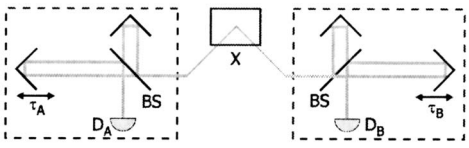

Fig. 1. Simplified scheme of the double Fourier spectrometer applied to a source X of photon pairs. The photons enter interferometers with independently adjusted optical delays τ_A and τ_B and are counted by detectors D_A and D_B.

0146-9592/06/081130-3/$15.00

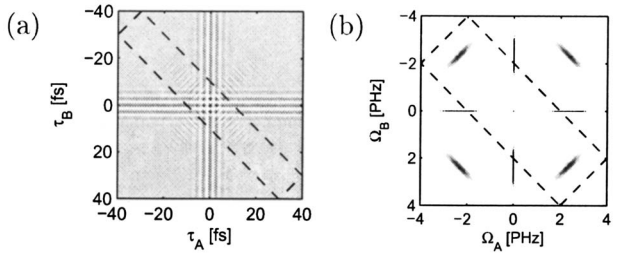

Fig. 2. (a) Typical coincidence interferogram as a function of optical path differences τ_A and τ_B and (b) its Fourier transform. The dashed rectangle in (a) defines the scan range, which with suitable sampling density yields the region of interest in the frequency domain, outlined in (b).

The measurement is carried out in the regime when the response time of the detector is much longer than the inverse of the smallest bandwidth characterizing the spectrum of the source. Then the only relevant characteristic of the source is the joint spectral intensity given by $\langle{:}\hat{I}_A(\omega_A)\hat{I}_B(\omega_B){:}\rangle$, where $\hat{I}_i(\omega_i)$ $(i=A,B)$ are the spectral intensity operators for beams A and B, and $\langle{:}\cdots{:}\rangle$ denotes the quantum mechanical expectation value of normally ordered operators. For a photon with a well-defined frequency ω, the probability of reaching the detector is given by the standard expression $(1+\cos\omega\tau_i)/2$. Consequently, the probability $p_{AB}(\tau_A,\tau_B)$ of a coincidence event for a source with an arbitrary spectrum takes the form

$$p_{AB}(\tau_A,\tau_B) \propto \frac{1}{4}\int \mathrm{d}\omega_A \int \mathrm{d}\omega_B \langle{:}\hat{I}_A(\omega_A)\hat{I}_B(\omega_B){:}\rangle \times(1+\cos\omega_A\tau_A)(1+\cos\omega_B\tau_B). \quad (1)$$

An example of the coincidence interferogram is shown in Fig. 2(a). The two-dimensional Fourier transform of the coincidence probability $p_{AB}(\tau_A,\tau_B)$ comprises the following terms:

$$\int \mathrm{d}\tau_A \mathrm{d}\tau_B p_{AB}(\tau_A,\tau_B)\exp(i\Omega_A\tau_A + i\Omega_B\tau_B) \propto \delta(\Omega_A)\delta(\Omega_B)\langle{:}\hat{N}_A\hat{N}_B{:}\rangle + \frac{1}{2}\delta(\Omega_A)\langle{:}\hat{N}_A\hat{I}_B(|\Omega_B|){:}\rangle + \frac{1}{2}\delta(\Omega_B)\langle{:}\hat{I}_A\delta(|\Omega_A|)\hat{N}_B{:}\rangle + \frac{1}{4}\langle{:}\hat{I}_A(|\Omega_A|)\hat{I}_B(|\Omega_B|){:}\rangle, \quad (2)$$

where $\hat{N}_i=\int \mathrm{d}\omega \hat{I}_i(\omega)$ is the operator of the total photon flux in the ith beam, $i=A,B$. The first term, localized at $\Omega_A=\Omega_B=0$, is proportional to the total number of photon pairs. The two middle terms lie on the axes $\Omega_A=0$ or $\Omega_B=0$ and have the shape of the single-photon spectra conditioned upon the detection of the conjugate photon. Finally, the last term contains the sought joint two-photon spectrum. For optical fields, these terms occupy distinct regions in the Ω_A,Ω_B plane and can be easily distinguished, as shown in Fig. 2(b). It is helpful to trace the origin of the four terms on the right-hand side of relation Eq. (2) to the coincidence interferogram. The vertical and the horizontal fringes generate the terms $\delta(\Omega_A)\times\langle{:}\hat{N}_A\hat{I}_B(|\Omega_B|){:}\rangle$ and $\delta(\Omega_B)\langle{:}\hat{I}_A(|\Omega_A|)\hat{N}_B{:}\rangle$, whereas it is the diagonal fringe pattern that contains information about the joint spectrum $\langle{:}\hat{I}_A(|\Omega_A|)\hat{I}_B(|\Omega_B|){:}\rangle$. This defines the region of the coincidence interferogram that needs to be scanned in order to compute the joint spectrum. It has the shape of a tilted rectangle outlined in Fig. 2(a). Let us note that the grid spacing in a given direction can be adjusted to the characteristic scale of interferogram structures. Specifically, the grid can be sparse in the direction parallel to the fringes, while in the perpendicular direction it needs to be fine enough to resolve the oscillations. Then the Fourier transform of the experimental data covers the region marked with a dashed rectangle in Fig. 2(b) that contains the joint spectrum.

Our experimental setup is depicted in Fig. 3(a). The photon pairs were generated in a 1 mm thick nonlinear BBO crystal in a type-I process. The crystal was pumped by 100 fs long pulses centered at 390 nm, with 20 mW average power, and a repetition rate of 80 MHz. The ultraviolet beam was focused on the crystal to a spot measured to be 155 μm in diameter. The crystal was cut at 29.7° to the optic axis and oriented perpendicular to the pump beam. Two Mach–Zehnder interferometers, MZ1 and MZ2, collected downconverted light at angles 1.28° and 1.05°. The photons transmitted through the interferometers were coupled into single-mode fibers defining the spatial modes in which the downconversion is collected.[12] Finally the photons were detected by using single-photon counting modules (SPCM) connected to fast coincidence electronics and a personal computer (PC) controlled counter board.

In order to ensure the stability of the interferometric setup over the entire two-dimensional scan we used a pair of common-path Mach–Zehnders, in which the two arms were implemented as orthogonal polarization components while the optical path difference was modulated by a Soleil compensator, as depicted in Fig. 3(b). The generated photons entered from the left, with their polarization set to 45° by the

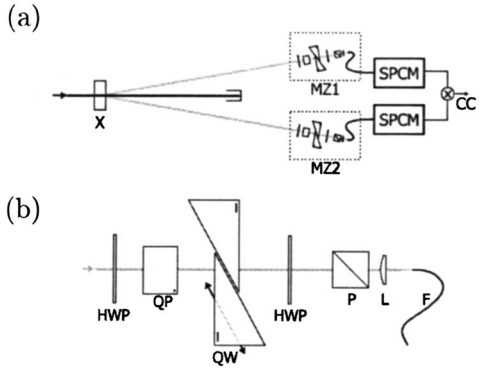

Fig. 3. (a) Experimental setup. X, BBO crystal; MZ1, MZ2, Mach–Zehnder interferometers; SPCM, single photon counting module, (b) Common-path Mach–Zehnder interferometer. HWP, half-wave plate; QP, quartz plate; QW, quartz wedges; P, polarizer; L, aspheric lens; F, single-mode fiber.

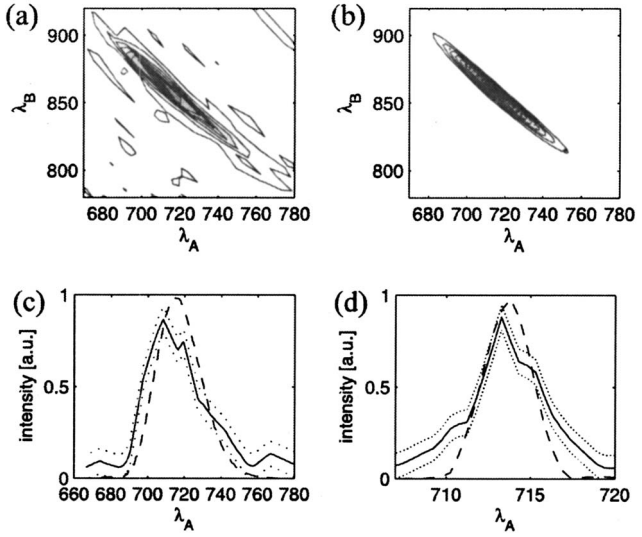

Fig. 4. (a) Measured joint spectrum of photon pairs $\langle :\hat{I}_A(\lambda_A)\hat{I}_B(\lambda_B):\rangle$ as a function of the wavelengths λ_A and λ_B; (b) theoretical predictions of the joint spectral intensity; cross sections of the theoretical (dashed curve) and the experimental (solid curve with dots marking errors) distributions along the lines (c) $\lambda_A^{-1}+\lambda_B^{-1}$= constant and (d)$\lambda_A^{-1}-\lambda_B^{-1}$ = constant passing through the maximum.

half-wave plate (HWP). Then the photons went through a block of crystalline quartz (QP) with a vertical optic axis and a pair of quartz wedges (QW) with horizontal optic axes. With this setup, the sign and the value of the delay between the horizontal and the vertical polarization components could be accurately controlled by sliding one of the wedges, mounted on the stepper motor-driven translation stage, into the beam. Finally, the two polarizations were brought to interference by using a second half-wave plate HWP and a polarizing beam splitter P, and the transmitted photons were coupled into a single-mode fiber F by using aspheric lens L and were detected. We verified that for the spectral range of interest birefringence dispersion could be neglected, and consequently the delays τ_i were linearly dependent on the displacements of the quartz wedges. The quartz blocks used in the setup allowed us to vary the delays from −250 to 250 fs.

The complete measurement consisted in a scan of a rectangular grid depicted in Fig. 1(a) spanned by 800×40 points, where the first number refers to the direction perpendicular to the fringes. The corresponding mesh was $0.57\ \text{fs}\times2$ fs, and coincidences were counted for 3 s at each point. The reconstructed joint spectrum of photon pairs, normalized to unity, is depicted in Fig. 4(a). We compare it with the theoretical calculations plotted in Fig. 4(b). The theoretical model used in these calculations assumed the exact phase matching function of the nonlinear crystal. The transverse components of the wave vectors for the pump and downconverted beams were treated in the paraxial approximation. The joint spectrum was calculated for coherent superpositions of plane-wave components of the downconversion light that add up to localized spatial modes defined by the collecting optics and single-mode fibers. In order to facilitate a more quantitative comparison, Figs. 4(c) and 4(d) show the cross sections of the joint spectra along directions of maximum and minimum widths in the frequency domain. In these plots, the experimental data have been interpolated between the points of the Fourier-domain grid and presented together with the statistical errors calculated assuming Poissonian noise affecting coincidence counts.

In summary, we proposed to use Fourier spectroscopy for measuring the joint spectrum of photons pairs and demonstrated its application to downconverted light generated in a type-I BBO crystal. The result of the reconstruction agrees well with a careful theoretical calculation of the joint spectrum. We were able to reduce substantially the overall duration of the measurement by selecting the region of the interferogram that contains information about the relevant characteristics of the spectrum. Finally, we note that, compared with scanning spectrometers, Fourier spectroscopy exhibits a higher signal-to-noise ratio when detection noise is dominated by an additive contribution. This effect, known as the multiplex advantage,[13] is important in the case of high dark count rates, which are typical for single-photon measurements performed at telecom wavelengths.[1]

This research was in part supported by Ministry of Education and Science grant 2P03B 029 26 and the EU project Qubit Applications (QAP, contract 015848). It has been carried out in the National Laboratory for Atomic, Molecular, and Optical Physics in Toruń, Poland. P. Wasylczyk acknowledges the support of the Foundation for Polish Science (FNP) during this work. W. Wasilewski's e-mail address is wwasil@fuw.edu.pl.

References

1. N. Gisin, G. Ribordy, W. Tittel, and H. Zbinden, Rev. Mod. Phys. **74**, 145 (2002).
2. V. Giovannetti, S. Lloyd, and L. Maccone, Nature **412**, 417 (2001).
3. A. Valencia, G. Scarcelli, and Y. Shih, Appl. Phys. Lett. **85**, 2655 (2004).
4. M. B. Nasr, B. E. A. Saleh, A. V. Sergienko, and M. C. Teich, Phys. Rev. Lett. **91**, 083601 (2003).
5. P. Walther, K. J. Resch, T. Rudolph, E. Schenck, H. Weinfurter, V. Vedral, M. Aspelmeyer, and A. Zeilinger, Nature **434**, 169 (2005).
6. C. Kurtsiefer, M. Oberparleiter, and H. Weinfurter, Phys. Rev. A **64**, 023802 (2001).
7. A. B. U'Ren, K. Banaszek, and I. A. Walmsley, Quantum Inf. Comput. **3**, 480 (2003).
8. F. König and F. N. C. Wong, Appl. Phys. Lett. **84**, 1644 (2004).
9. J. P. Torres, F. Macia, S. Carrasco, and L. Torner, Opt. Lett. **30**, 314 (2005).
10. P. S. K. Lee, M. P. van Exter, and J. P. Woerdman, Phys. Rev. A **72**, 033803 (2005).
11. Y.-H. Kim and W. P. Grice, Opt. Lett. **30**, 908 (2005).
12. A. Dragan, Phys. Rev. A **70**, 053814 (2004).
13. M. H. Tai and M. Harwit, Appl. Opt. **15**, 2664 (1976).